ChemComm

COMMUNICATION

A highly emissive and stable zinc(II) metal–organic framework as a host–guest chemopalette for approaching white-light-emission†

Hong Cai,[ab] Li-Li Xu,[ab] He-Yun Lai,[a] Jing-Yi Liu,[b] Seik Weng Ng[c] and Dan Li *[d]

Cite this: *Chem. Commun.*, 2017, 53, 7917

Received 30th April 2017,
Accepted 17th June 2017

DOI: 10.1039/c7cc03350h

rsc.li/chemcomm

A new adenine-containing metal–organic framework (MOF), [Zn_4O-(adenine)$_4$(benzene-1,3-dicarboxylate)$_4Zn_2$] (named as ZnBDCA), was synthesized solvothermally. ZnBDCA possesses high quantum yield (>50%) and nano-channels that can encapsulate acriflavine molecules to build a host–guest chemopalette for approaching white-light emission.

Metal–organic frameworks (MOFs) are emerging as promising crystalline porous materials composed of multitopic organic struts linking metal-based nodes.[1] They have attracted considerable attention in many fields such as gas storage and separation,[2] catalysis,[3] sensors,[4] and luminescent materials[5] due to their permanent porosity and rich host–guest interactions. Among more than 60 000 MOFs which are included in the Cambridge Structural Database (CSD), only about 10% MOFs reveal luminescence properties. And many of them have low quantum yields of typically <20%.[6] It is noteworthy that most reports focus on rare-earth (RE)-base MOFs or RE-doped MOFs.[7] However, as the demand of RE elements continuously increases in the high-tech applications, the scarce resources and high prices of RE have pushed the search for alternative RE-free luminescent materials to a level of high importance.

Metal complexation especially with a core–shell structure can significantly enhance their stabilities and luminescence properties.[8,9] Vogler and Kunkely first found that solutions of $Zn(O_2CMe)_2$ did not show any photoluminescence, but solutions of $[Zn_4O(O_2CMe)_6]$ emitted an intense photoluminescence because of its core–shell structure.[8b,c] In the early 90s the group of Che,[9] selecting $[Zn_4O(O_2CMe)_6]$ as a molecular model, reported a compound $[Zn_4O(AID)_6]$ (Fig. 1a and Fig. S5 in the ESI†) that featured a tetrameric zinc(II) cluster with 7-azaindolate core–shell structure. This complex possessed high-efficiency emission, and was demonstrated to be an emitter in OLEDs a few years later.[9c] In 2015, the group of Che adopted 2-(2-hydroxyphenyl)benzothiazolate which is the derivate of 7-azaindolate as a ligand to prepare Zn-1. This complex is isostructural with $[Zn_4O(AID)_6]$. And the emission quantum efficiency of the Zn-1 thin film is up to 96%.[9d] Herewith, we put forward a strategy using the tetrameric zinc(II) cluster core–shell structure as a building block to construct highly emissive MOFs, and efficient white-light emission was achieved by

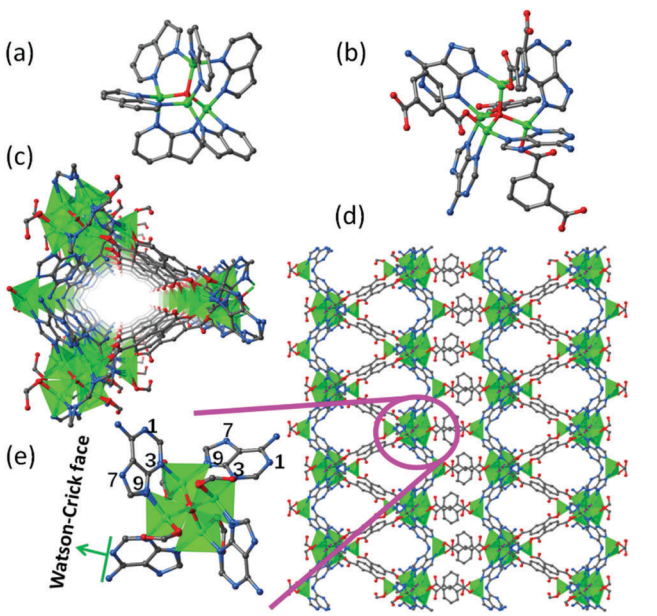

Fig. 1 (a) $[Zn_4O(AID)_6]$ core–shell structure and (b) $[(Zn_4O)(ade)_4(BDC)_4Zn_2]$ core–shell structure. (c) The 1D channel of the ZnBDCA. (d) Perspective view of the overall framework of ZnBDCA along the *b* axis. (e) $Zn_4O(ade)_4(COO)_4$ cluster with Watson–Crick face. Color codes: C, dark grey; N, blue; O, red; Zn, green (tetrahedra); H omitted.

[a] *School of Chemistry and Environmental Engineering, Hanshan Normal University, Chaozhou, Guangdong 521041, P. R. China*
[b] *Department of Chemistry, Shantou University, Guangdong 515063, P. R. China*
[c] *The University of Nottingham Malaysia Campus, 43500 Semenyih, Selangor, Malaysia*
[d] *College of Chemistry and Materials Science, Jinan University, Guangzhou, Guangdong 510632, P. R. China. E-mail: danli@jnu.edu.cn*

† Electronic supplementary information (ESI) available: Experimental details, crystal data, physical measurements. CCDC 1545843. For ESI and crystallographic data in CIF or other electronic format see DOI: 10.1039/c7cc03350h

encapsulating guests in the MOF cavity by means of a complementary colour approach termed as a chemopalette.[10]

Obviously, 7-azaindole[11a] is not a suitable ligand to form three-dimensional MOFs, because pyrimidine N and imidazole N of the 7-azaindole have been occupied by Zn. There are no redundant coordination atoms to link the other Zn_4O cluster. As we know, adenine and 7-azaindole are bioisosteres with a lot of resemblance. Adenine has more coordination sites and can self-associate *via* hydrogen bonding in solution, and the nonradiative decay pathway can be blocked by bonding to the metal center.[11] We chose adenine with a Zn_4O cluster to create a core–shell secondary building unit (SBU). In order to increase the dimension of MOFs, benzene-1,3-dicarboxylate (BDC) as the auxiliary ligand was used to connect the other SBUs to form a 3D MOF (Fig. 1b and Fig. S5, ESI†) because of the similar coordination model and the orbital complementarity of the μ-carboxylato-κO:κO′ and μ-adenine-κN_3:κN_9 bridging ligands.[11e]

Here, we synthesized a new adenine-containing MOF with Zn_4O core–shell structure *via* a solvothermal method, $[(Zn_4O)(ade)_4(BDC)_4Zn_2]\cdot 6DMF\cdot 4H_2O$, heretofore referred to as ZnBDCA (ade = adenine; BDC = benzene-1,3-dicarboxylate). The formula of ZnBDCA was established based on the single-crystal X-ray structure, elemental analysis, and thermogravimetric analysis (Fig. 1 and Fig. S1, S5, ESI†).

Single-crystal X-ray diffraction analysis revealed that ZnBDCA crystallized in the $P\bar{4}2_1c$ space group (see the ESI† for crystal data, Table S1 and Fig. S5) and contained two crystallographically independent Zn centres, all with tetrahedral coordination geometry. Four Zn^{2+} are quadruply bound by N3 and N9 from two adenines, monodentate carboxyl groups and the central oxygen atom, respectively, and to form a $Zn_4O(ade)_4(COO)_4$ SBU (Fig. 1e), which is extended *via* linking the monodentate carboxyl groups of BDC. The $Zn_4O(AID)_6$ core–shell structure seems to be well suited as a model for the $Zn_4O(ade)_4(COO)_4$ cluster SBU since the important structural features of both structures are very similar.[8] Even the Zn–O (*ca.* 1.90–1.98 Å) and Zn–Zn (3.1–3.20 Å) bond distances for both compounds are almost identical. This SBU is further extended through coordinating with the other Zn^{2+}, which is completed by two monodentate carboxyl O and two adenine N (N7) to construct the overall framework with large 1D channels (Fig. 1c). The channel is tetragonal and the diameter is about 10 Å. The vacancies are filled with DMF and water molecules. The total solvent accessible volume calculated using PLATON is 30.2% of the unit cell volume. From the perspective view of the overall framework, ZnBDCA looks like a DNA helix connected by metal ions along the *b* axis resulting in high helix stability (Fig. 1d). Fortunately, it is found that the interior surface of the ZnBDCA framework is decorated with exposed open Watson–Crick sites and uncoordinated carboxyl O donors, which are prone to rich host–guest recognition.

Both the thermal stability and solvent resistance of ZnBDCA are very high. The unchanged pattern of powder X-ray diffraction (PXRD) confirmed that the framework structure remained intact after the as-synthesized sample was heated at 400 °C in air, or immersed in organic solvents for several weeks (Fig. S1–S4, ESI†).

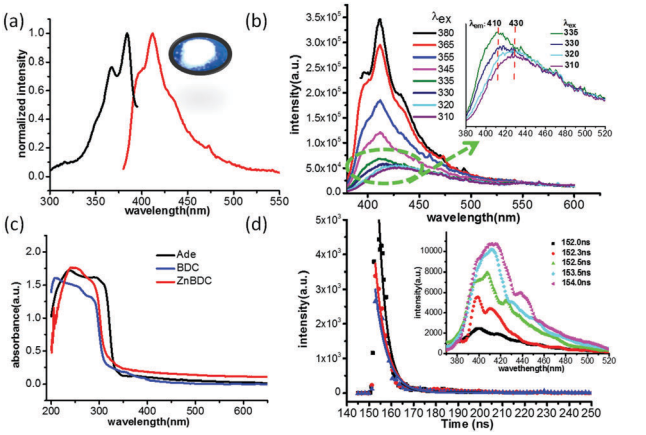

Fig. 2 (a) Excitation (black) and emission (red) spectra of ZnBDCA. (b) Emission spectra of ZnBDCA with different excitation wavelengths (inset: enlarge λ_{ex} = 335–310 nm). (c) UV-Vis spectra of ZnBDCA (red), BDC (blue) and adenine (black) in the solid state. (d) Luminescence decay curves measured for the ZnBDCA powder sample at 77 K. Black points for monitoring at 400 nm; red points for monitoring at 410 nm; blue points for monitoring at 430 nm; all solid lines through the experimental points were calculated using single exponential decay function. Inset: Time-resolved luminescence spectra of the ZnBDCA powder sample.

High stability is very important for permanently porous materials in practical applications.

As expected, ZnBDCA emitted very intense photoluminescence in the solid state under UV light irradiation at room temperature with an average quantum efficiency of 53% (excited at 360 nm). Fig. 2a shows the emission spectrum, where the maximum excitation wavelength is 380 nm, and the maximum emission wavelength of ZnBDCA is located at about 410 nm with two shoulders at around 400 nm and 430 nm. Interestingly, upon decreasing the excitation wavelengths, the maximum emission peak at 410 nm was broadened. When the excitation wavelength is $<$330 nm, the maximum emission wavelength of ZnBDCA shifts from 410 nm to 430 nm (Fig. 2b). To confirm the origin of the blue-violet emission, the emission spectra of free BDC and adenine were measured under the same conditions (Fig. S7, ESI†). The maximum peak wavelengths of free BDC and adenine are approximately 400 nm and 430 nm, respectively. Therefore, we reasonably believe that the emission of ZnBDCA at about 430 nm can be assigned to the adenine intraligand π–π* transition, and the high-energy emission at about 400 nm can be assigned to the BDC intraligand π–π* transition, because the free adenine and BDC ligands exhibit the same emission. This means that ZnBDCA actually retained the properties of the ligands. The maximum emission peak at about 410 nm is most likely due to the ligand-to-metal charge-transfer (LMCT) around the $Zn_4O(ade)_4(COO)_4$ cluster, other than the possible interligand transitions of adenine and BDC. The luminescence behaviour is very similar to that of MOF-5, which consists of metal clusters of $[Zn_4O]$ connected by benzene dicarboxylate linkers to form a 3D structure, and the green emission originated from the photo-induced electron transfer from the terephthalate antenna to the $Zn_4O(COO)_6$ core–shell cluster.[8e,f] Adenine phototautomerizes *via* the proton-coupled electron transfer (PCET) process, and the

most significant nonradiative pathway is associated with its imidazole N proton and is at least partly pertinent to excited-state proton transfer processes.[10b] However, when Zn(II) is bonded with the imidazole N, the nonradiative decay pathway can be blocked. Moreover, the $Zn_4O(ade)_4(COO)_4$ cluster is connected by BDC forming a 3D MOF, through photoinduced electron transfer from the BDC antenna to the $Zn_4O(ade)_4(COO)_4$ cluster core–shell cluster.

To prove the above speculation, the UV-Vis absorption spectra of ZnBDCA, adenine and BDC were measured (Fig. 2c). The absorption spectrum featured intense broad bands centred at 240–290 nm and a broad shoulder at around 330 nm for ZnBDCA. The bands at 240–290 nm are assigned to the interaction between the two ligands, since ultraviolet absorption peaks represent for free BDC (205–290 nm) and adenine (235–325 nm). The broad shoulder at 330 nm in the ZnBDCA absorption spectrum is most likely due to the interaction between adenine and/or the BDC ligand that surround the Zn_4O core–shell cluster.

To further demonstrate the conjecture, time-resolved fluorescence decay profiles of a ZnBDCA solid sample pumped by 337 nm pulses at 77 K are shown in Fig. 2d. The decay dynamics were monitored at 400 nm, 410 nm and 430 nm, and the lifetime values are about 1.5 ns, 4.8 ns and 3.7 ns observed by single-exponential fitting, respectively. This can be seen more clearly in the time-resolved spectra (Fig. 2d inset and Fig. S8, ESI†). Initially the emissions around 400 nm and 420 nm appear. This is due to that the low intensity makes the two peaks at 410 and 430 nm merge together (see the dotted black line). After 300 ps, weak as it is, the shoulder peak at about 430 nm is discernible with increasing the intensity of 400 nm and 410 nm (see the dotted red line). Soon afterwards, the peak at 430 nm gradually increases (see the dotted green line), then gradually red shifts to 440 nm (see the dotted cyan and purple lines). This phenomenon is very similar to that of the time-resolved luminescence spectra of $[Zn_4O(AID)_6]$,[9b] the emission of which is due to LMCT around the Zn_4O core–shell structure. It is reasonable to conclude that the emission of ZnBDCA is attributed to the LMCT around the Zn_4O cluster and the interligand/intraligand adenine and BDC charge transition.

Besides the metal centres/cluster and organic linkers that can produce emission, guest molecules can also generate luminescence.[12] The well-established host–guest interaction can be utilized to construct white-light-emitting supramolecular systems with high quantum yield. In order to improve the light emission efficiency and control emission colour of ZnBDCA, acriflavine fluorescent molecules were introduced into the porous MOF (Fig. S9, ESI†), denoted as Acf@ZnBDCA.

We chose acriflavine as a guest for the following reasons: firstly, adenine-based ZnBDCA features the open Watson–Crick sites, retaining some properties of adenine. There is heterogeneity of the interaction between DNA and acriflavine.[13a] So, ZnBDCA and acriflavine are prone to form interactions through host–guest recognition.[13] Secondly, the molecular size of acriflavine is about $10.5 \times 5.04 \times 3.79$ Å^3. And the accessible space of ZnBDCA (the channel diameter is about 10×10 Å^2) is big enough to accommodate acriflavine as a guest. Thirdly, acriflavine

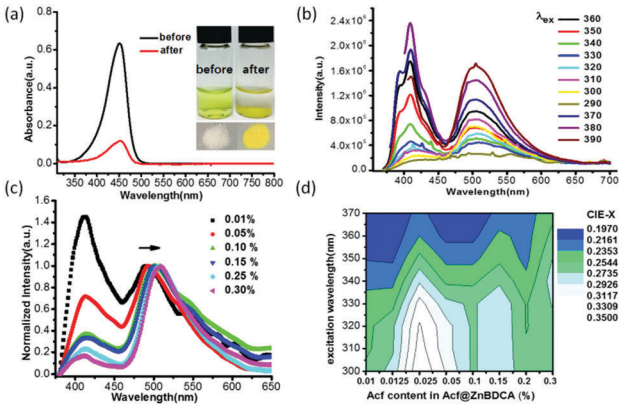

Fig. 3 (a) UV-Vis spectra of acriflavine solution immersed in ZnBDCA, before and after. The photographs show the colours of dyes before and after adsorption. (b) Emission spectra of Acf@ZnBDCA (Acf concentration is 0.05 wt%) excited at different wavelengths in the solid state at room temperature. (c) Emission spectra of Acf@ZnBDCA with different amounts of encapsulated acriflavine (λ_{ex} = 320 nm). (d) 2D matrix models correlating CIE coordinates with different amounts of encapsulated acriflavine for Acf@ZnBDCA excited from 370 nm to 300 nm at room temperature.

emits a bright yellow-green light and ZnBDCA emits a bright blue-violet light, thus the combination of the host and the guest may produce a white light emission based on the principle of complementary colour.

In order to verify the feasibility of this strategy, ZnBDCA crystals were soaked in acriflavine aqueous solutions in a sample vial at room temperature to prepare a host–guest supramolecular system. The colourless samples at the bottom of the vial became yellow. This was not only observed by the naked eye but also proved by the dramatic decline in the UV-Vis absorption spectrum of the supernatant fluid (Fig. 3a). Both the solid-state UV-Vis absorption spectrum and the diffuse reflection spectrum of Acf@ZnBDCA showed the characteristic absorption peak at 460 nm, which proved that the acriflavine guest had been encapsulated in ZnBDCA (Fig. S10, ESI†). The N_2 and CO_2 adsorption isotherms of ZnBDCA and Acf@ZnBDCA showed that both the N_2 and CO_2 uptakes of Acf@ZnBDCA were lower than those of ZnBDCA (Fig. S11, ESI†). This can further prove that the acriflavine molecule has entered into the nano-channels.

Acf@ZnBDCA displayed strong luminescence and simultaneously showed both the characteristic emissions of the guest ($\lambda_{em} \approx 510$ nm) and host moieties ($\lambda_{em} \approx 410$ nm) upon excitation at 370 nm (Fig. S12, ESI†). Interestingly, Acf@ZnBDCA can systematically adjust the emissive light colour by changing the excitation wavelength (Fig. S13 and S14, ESI†) realized as the chemopalette strategy[10] from a host–guest system. The intensity ratio of the host and guest can be changed by being excited at different wavelengths (Fig. 3b), thereby changing the emission colour from blue to yellow. Moreover, the emission intensity of acriflavine is significantly enhanced with increasing the amounts of encapsulated acriflavine in the Acf@ZnBDCA system (Fig. 3c). From the 2D matrix models correlating CIE coordinates (Fig. 3d and Fig. S15, ESI†), changing the excitation wavelength and modulating the amounts of acriflavine can readily

produce white light emission. For example, when the concentration of acriflavine in the Acf@ZnBDCA system was 0.12 wt% and the material was excited at 320 nm, the corresponding CIE coordinates (0.313, 0.347) would be obtained. Surprisingly, the maximum quantum yield of Acf@ZnBDCA was about 32%, which is decreased as compared with that of ZnBDCA. Notably, the emission peak of acriflavine red shifted from 490 nm to 510 nm when the amounts of the dye in Acf@ZnBDCA increased (Fig. 3c). Therefore, there must be interesting host–guest interaction between the adenine-based MOF and the acriflavine DNA-stain, and energy transfer occurred in the excited state of the Acf@ZnBDCA system (Fig. S16, ESI†).

The stability of Acf@ZnBDCA was also examined. According to the TGA results, the decomposition temperature of Acf@ZnBDCA did not decrease as compared with that of ZnBDCA (Fig. S17, ESI†). The position of PXRD did not change at 400 °C, which further confirmed that the system had high thermostability (Fig. S18, ESI†).

In conclusion, a new nucleobase-containing MOF (named as ZnBDCA) with a core–shell molecular structure was successfully prepared, which possesses high quantum yield of 53%. The emission of ZnBDCA is attributable to the LMCT around the Zn_4O cluster and the interligand/intraligand adenine and BDC charge transition. Thus, this approach would be a very promising strategy to develop high-emission luminescent MOFs. Moreover, the nano-channeled framework of ZnBDCA bears the open Watson–Crick sites which are prone to encapsulate acriflavine molecules and form an Acf@ZnBDCA supramolecular system. The system, as a MOF-dye host–guest chemopalette, emits bright cool white-light by changing the excitation energy or by modulating the amounts of the encapsulated guest. These results will further facilitate the investigation of such MOFs as new types of functional materials for applications in biological and optical materials.

This work was financially supported by the National Basic Research Program of China (No. 2013CB834803), the National Natural Science Foundation of China (No. 91222202 and 21171114) and Scientific Research Start-up Funds of Hanshan Normal University (QD20161009).

Notes and references

1 (*a*) H.-C. Zhou, J. R. Long and O. M. Yaghi, *Chem. Rev.*, 2012, **112**, 673; (*b*) T. R. Cook, Y.-R. Zheng and P. J. Stang, *Chem. Rev.*, 2013, **113**, 734.

2 (*a*) Q. Yang, D. Liu, C. Zhong and J.-R. Li, *Chem. Rev.*, 2013, **113**, 8261; (*b*) M. P. Suh, H. J. Park, T. K. Prasad and D.-W. Lim, *Chem. Rev.*, 2012, **112**, 782; (*c*) J. B. DeCoste and G. W. Peterson, *Chem. Rev.*, 2014, **114**, 5695; (*d*) N. C. Burtch, H. Jasuja and K. S. Walton, *Chem. Rev.*, 2014, **114**, 10575.

3 (*a*) M. Rimoldi, A. J. Howarth, M. R. DeStefano, L. Lin, S. Goswami, P. Li, J. T. Hupp and O. K. Farha, *ACS Catal.*, 2017, **7**, 997; (*b*) Y. Zhao, *Chem. Mater.*, 2016, **28**, 8079; (*c*) A. Corma, H. García and F. X. Llabrés i Xamena, *Chem. Rev.*, 2010, **110**, 4606.

4 (*a*) A. M. Plonka, Q. Wang, W. O. Gordon, A. Balboa, D. Troya, W. Guo, C. H. Sharp, S. D. Senanayake, J. R. Morris, C. L. Hill and A. I. Frenkel, *J. Am. Chem. Soc.*, 2017, **139**, 599; (*b*) B. Li, H.-M. Wen, Y. Cui, W. Zhou, G. Qian and B. Chen, *Adv. Mater.*, 2016, **28**, 8819.

5 (*a*) Y. Cui, Y. Yue, G. Qian and B. Chen, *Chem. Rev.*, 2012, **112**, 1126; (*b*) Q. Zhang, C. Zhang, L. Cao, Z. Wang, B. An, Z. Lin, R. Huang, Z. Zhang, C. Wang and W. Lin, *J. Am. Chem. Soc.*, 2016, **138**, 5308.

6 (*a*) Q. Gong, Z. Hu, B. J. Deibert, T. J. Emge, S. J. Teat, D. Banerjee, B. Mussman, N. D. Rudd and J. Li, *J. Am. Chem. Soc.*, 2014, **136**, 16724; (*b*) Z. Wei, Z.-Y. Gu, R. K. Arvapally, Y.-P. Chen, R. N. McDougald, Jr., J. F. Ivy, A. A. Yakovenko, D. Feng, M. A. Omary and H.-C. Zhou, *J. Am. Chem. Soc.*, 2014, **136**, 8269.

7 (*a*) D. E. Barry, D. F. Caffrey and T. Gunnlaugsson, *Chem. Soc. Rev.*, 2016, **45**, 3244; (*b*) J. Rocha, L. D. Carlos, F. A. A. Paz and D. Ananias, *Chem. Soc. Rev.*, 2011, **40**, 926.

8 (*a*) C. Louis, S. Roux, G. Ledoux, C. Dujardin, O. Tillement, B. L. Cheng and P. Perriat, *Chem. Phys. Lett.*, 2006, **429**, 157; (*b*) A. Vogler and H. Kunkely, *Top. Curr. Chem.*, 2001, **213**, 143; (*c*) H. Kunkely and A. Vogler, *J. Chem. Soc., Chem. Commun.*, 1990, 1204; (*d*) Z. Li, Z. Gao, H. Wang, H. Zhang, X. Zhao, B. Mi and W. Huang, *Sci. China: Chem.*, 2012, **55**, 2562; (*e*) P. L. Feng, J. J. Perry IV, S. Nikodemski, B. W. Jacobs, S. T. Meek and M. D. Allendorf, *J. Am. Chem. Soc.*, 2010, **132**, 15487; (*f*) S. Bordiga, C. Lamberti, G. Ricchiardi, L. Regli, F. Bonino, A. Damin, K. P. Lillerud, M. Bjorgen and A. Zecchina, *Chem. Commun.*, 2004, 2300.

9 (*a*) C.-F. Lee, K.-F. Chin, S.-M. Peng and C.-M. Che, *J. Chem. Soc., Dalton Trans.*, 1993, 467; (*b*) Y. Ma, T. Lai and Y. Wu, *Adv. Mater.*, 2000, **12**, 433; (*c*) Y. Ma, C.-M. Che, H.-Y. Chao, X. Zhou, W.-H. Chan and J. Shen, *Adv. Mater.*, 1999, **11**, 852; (*d*) G. Cheng, G. K.-M. So, W.-P. To, Y. Chen, C.-C. Kwok, C. Ma, X. Guan, X. Chang, W.-M. Kwok and C.-M. Che, *Chem. Sci.*, 2015, **6**, 4623; (*e*) I. H. T. Sham, C.-C. Kwok, C.-M. Che and N. Zhu, *Chem. Commun.*, 2005, 3547.

10 (*a*) S.-Z. Zhan, M. Li, S. W. Ng and D. Li, *Chem. – Eur. J.*, 2013, **19**, 10217; (*b*) G. Liu, D.-Q. Feng, X. Mu, W. Zheng, T. Chen, L. Qi and D. Li, *J. Mater. Chem. B*, 2013, **1**, 2128.

11 (*a*) S.-B. Zhao and S. Wang, *Chem. Soc. Rev.*, 2010, **39**, 3142; (*b*) A. Domínguez-Martín, M. del P. Brandi-Blanco, A. Matilla-Hernández, H. El Bakkali, V. M. Nurchi, J. M. González-Pérez, A. Castiñeiras and J. Niclós-Gutiérrez, *Coord. Chem. Rev.*, 2013, **257**, 2814; (*c*) A. I. Kononov and M. N. Bukina, *J. Biomol. Struct. Dyn.*, 2002, **20**, 465; (*d*) S. R. Sushrutha, R. Hota and S. Natarajan, *Eur. J. Inorg. Chem.*, 2016, 2962; (*e*) G. Beobide, O. Castillo, J. Cepeda, A. Luque, S. Pérez-Yánez, P. Román and J. Thomas-Gipson, *Coord. Chem. Rev.*, 2013, **257**, 2716.

12 (*a*) M. D. Allendorf, M. E. Foster, F. Léonard, V. Stavila, P. L. Feng, F. P. Doty, K. Leong, E. Y. Ma, S. R. Johnston and A. A. Talin, *J. Phys. Chem. Lett.*, 2015, **6**, 1182; (*b*) M. C. So, G. P. Wiederrecht, J. E. Mondloch, J. T. Hupp and O. K. Farha, *Chem. Commun.*, 2015, **51**, 3501.

13 (*a*) R. K. Tubbs, W. E. Ditmars and Q. Van Winkle, *J. Mol. Biol.*, 1964, **9**, 545; (*b*) H. Cai, M. Li, X. R. Lin, W. Chen, G. H. Chen, X. C. Huang and D. Li, *Angew. Chem., Int. Ed.*, 2015, **54**, 10454; (*c*) L. M. Chan and Q. Van Winkle, *J. Mol. Biol.*, 1969, **40**, 491; (*d*) I. Isenberg, R. B. Leslie, S. L. Baird, Jr., R. Rosenbluth and R. Bersohn, *Proc. Natl. Acad. Sci. U. S. A.*, 1964, **52**, 379; (*e*) R. N. Dsouza, U. Pischel and W. M. Nau, *Chem. Rev.*, 2011, **111**, 7941.

